Latest Developments in Metalloenzyme Design and Repurposing

Tillmann Heinisch[a] and Thomas R. Ward*[a]

Abstract: In the past decade, artificial metalloenzymes have emerged has attractive alternatives to more traditional homogeneous catalysts and enzymes. This microreview presents a selection of recent achievements in the design of such hybrid catalysts. These include artificial Zn-hydrolases and metathesases, the heme-protein repurposing for C-H, N-H and S-H insertion reactions, novel light-driven redox hybrid catalysts, novel scaffold proteins and metallocofactor anchoring techniques and metalloenzyme models.

1. Introduction

The ever increasing wealth of structural and functional data accumulated for proteins encourages to probe and widen our knowledge of enzymes experimentally by creating artificial (metallo)enzymes (AME hereafter) or by exploring latent activities of natural metalloenzymes by redesign.[1,2] Designing proteins and hybrids for novel functions is not only a valuable exercise for academic research but holds promise for applications in medicine, synthesis and biotechnology. This microreview aims to provide insight into the latest examples of AME design and metalloenzyme repurposing including zinc hydrolases, novel C-H, N-H, S-H insertion reactions, light-driven redox reactions, novel protein scaffolds for metalloenzyme engineering and metallocofactor anchoring techniques, the *in vivo* application of AMEs and metalloenzyme models.

Thomas R. Ward obtained his PhD in chemistry at the ETHZ under the guidance of Profs. L-M Venanzi and D. Seebach. After postdocs with Roald Hoffmann and Carlo Floriani, he initiated his carreer in bioinorganic chemistry (University of Berne) and bio-inspired catalysis (University of Neuchatel). In 2008, he moved to the University of Basel and runs a group focusing on the exploitation of artificial metalloenzymes in vivo.

Tillmann Heinisch received his PhD in Chemistry and Protein Crystallography at the University of Basel under Prof. T. R. Ward and T. Schirmer. After joining the group of Prof. Frances Arnold at Caltech for postdoctoral research he returned to Basel for a second postdoc. His research interest is the structure-based engineering of artificial metalloenzymes.

[a] T., Heinisch, T. R. Ward
Department of Chemistry
University of Basel
Spitalstrasse 51, 4056 Basel, Switzerland
E-mail: Thomas.ward@unibas.ch

2. Zn-Hydrolases

Zn-hydrolases have attracted wide attention in the protein design community. This might relate to the abundance and fundamental functions of zinc-hydrolases in nature, the relative simplicity of the catalyzed hydrolysis reactions, the availability of structural and functional data for zinc hydrolases and the relative ease with which models of zinc hydrolases can be generated and evaluated.[3,4]

In many metalloenzymes, catalytic metals act as Lewis acids rather than redox-active cofactors (e.g. kinases, class 1 terpene synthases, peptidases). In zinc hydrolases, the metal adopts either a 4-coordinate tetrahedral or a 5-coordinate distorted-trigonal bipyramidal geometry and is often coordinated by lone pairs of nitrogen or oxygen of His, Glu or Asp side chains. Typically water occupies initially a remaining coordination site at the metal which results in a dramatic reduction of its pK_a value by 8 to 12 units in combination with H-bonding interactions of surrounding amino acids. The acidified water (or the corresponding hydroxo) attacks an electrophilic function of the substrate such as a carbonyl or phosphonate group leading to the formation of a negatively charged tetrahedral or trigonal-bipyramidal intermediate or transition state, respectively. The intermediate is frequently stabilized by a positively charged or polarized “oxyanion hole” provided by proximal protein residues. The scissile C-O, C-N or P-O bond is subsequently cleaved and the two products are released. Enhanced nucleophilicity of coordinated water through Lewis acid coordination can be operational in ester, amide and phosphoester hydrolysis but also in addition reactions such as the hydration of carbon dioxide or enones.

In Nature, Zn^{II} ions are coordinated to side chains of amino acids that are part of distinct secondary structural motifs such as β-sheets or α-helices. In a *de novo* approach, Pecoraro and coworkers computationally designed a peptide that assembles into a 3-α-helical bundle and is stabilized upon Zn^{II} ion coordination through a $(His)_3$ motif. Zinc is located at one end of the resulting bundle and each His is located on an individual α-helix (Figure 1).[5] The 3-helix bundle is stabilized on the opposite end by a Hg^{II} ion coordinated to a $(Cys)_3$ motif. The crystal structure of the resulting hybrid catalyst showed that the catalytic Zn^{II}-bound water in the center of the bundle was virtually superimposable with the corresponding $(His)_3(H_2O)Zn^{II}$ site in human carbonic anhydrase II (hCAII hereafter). In CO_2 hydration, the catalyst has a very high catalytic constant (k_{cat}) of 1800 s^{-1}, which is only 100-fold smaller than that of natural hCAII, and a Michaelis constant (K_M) 10-fold lower than that of hCAII.

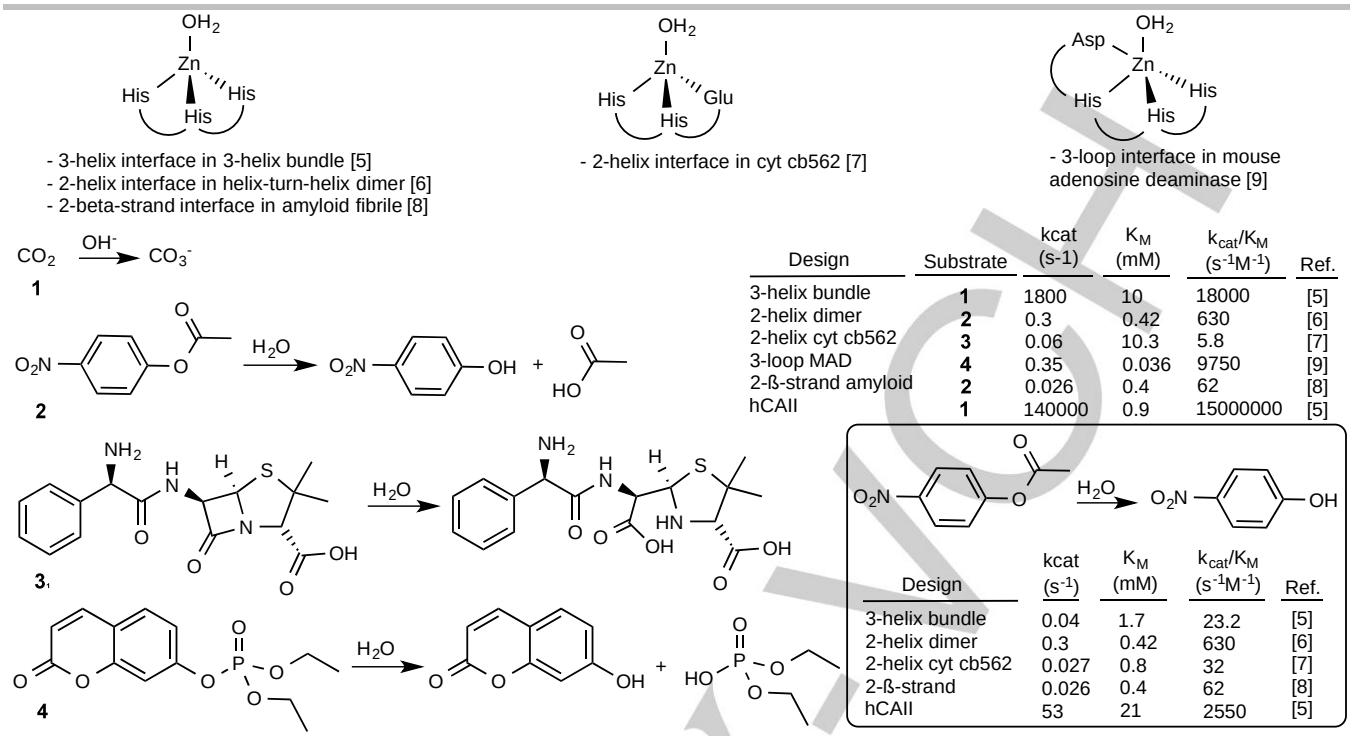

Design	Substrate	kcat (s-1)	K_M (mM)	k_{cat}/K_M ($s^{-1}M^{-1}$)	Ref.
3-helix bundle	**1**	1800	10	18000	[5]
2-helix dimer	**2**	0.3	0.42	630	[6]
2-helix cyt cb562	**3**	0.06	10.3	5.8	[7]
3-loop MAD	**4**	0.35	0.036	9750	[9]
2-ß-strand amyloid	**2**	0.026	0.4	62	[8]
hCAII	**1**	140000	0.9	15000000	[5]

Design	kcat (s^{-1})	K_M (mM)	k_{cat}/K_M ($s^{-1}M^{-1}$)	Ref.
3-helix bundle	0.04	1.7	23.2	[5]
2-helix dimer	0.3	0.42	630	[6]
2-helix cyt cb562	0.027	0.8	32	[7]
2-ß-strand	0.026	0.4	62	[8]
hCAII	53	21	2550	[5]

Figure 1. Artificial Zn-hydrolases.

Kuhlman and coworkers engineered the interface of a computationally designed homodimer of a helix-turn-helix protein to bind zinc to an engineered $(His)_3$ motif.[6] The hybrid catalyst was structurally characterized and displays *p*-nitrophenol acetate (*p*NPA hereafter) hydrolase activity. A 50-fold decreased K_M for this reaction vs. hCAII indicated strong substrate binding but a k_{cat} of 0.3 s^{-1} resulted in a limited catalytic efficiency.

An α-helical fold was the template of an artificial Zn-hydrolase engineered by Tezcan and coworkers.[7] In a related approach to Kuhlman *et al.*, they modified surface residues that triggered a monomeric cytochrome P450 cb562 to form a D2 symmetrical homotetramer stabilized by disulfide bridges as well as hydrophobic and metal coordinating interactions. Additional positioning of a $(His)_2Glu$ motif into the surface exposed fraction of a monomer-monomer interface allowed binding of a second Zn^{II} ion as a catalytic center upon decreasing the bulk at positions K104A and E57G. Substrates *p*NPE and ampicillin were hydrolyzed by the designer enzyme with catalytic efficiencies of 32 and 5.8 $s^{-1}M^{-1}$, respectively. The *in vivo* compatibility of this artificial ampicillinase was demonstrated by periplasmic expression in *E. coli*, which enabled cell growth on ampicillin-supplemented agar.

Although α-helical proteins predominate the field of artificial Zn-hydrolases, Korendyrovych and coworkers could demonstrate that a $(His)_3Zn^{II}$ catalytic site can be engineered into the strand-strand interface of a β-sheet which is reminiscent of the hCAII active site. The authors exploited the self-assembly of short peptides into amyloid fibrils to design a moderately active Zn-hydrolase.[8]

Natural zinc sites can also be repurposed for novel function. Baker, Tawfik and coworkers used the RosettaDesign algorithm to screen an *in silico* designed theozyme against the protein data bank (PDB hereafter) for Zn-proteins with potential activity in hydrolysis of organophosphonate nerve agents. The authors identified mouse adenosine deaminase to display hydrolysis activity for a colorimetric organophosphonate substrate surrogate upon introduction of the residues suggested by RosettaDesign (Figure 1, substrate **4**).[9] After three rounds of directed evolution the catalytic efficiency of the initial computational design was 2500-fold improved, almost exclusively by an increase in k_{cat}.

3. New Reactions

AME design has the potential to expand Nature´s enzymatic reaction repertoire by introducing abiotic catalytic entities developed that have no equivalent among natural enzymes. We summarize below the latest additions to the portfolio of AME-catalyzed reactions.

3.1. Metathesases

Olefin ring-closing metathesis (RCM) is a widely applicable and selective reaction for the intramolecular formation of internal C=C double bonds from olefins (Figure 2). One of the most widely used catalysts is the Grubbs-Hoyveda 2nd generation ruthenium complex. Importantly, it is water compatible, albeit with reduced productivity.[10,11] Several groups set out to investigate if the catalyst can be anchored to a protein and if the protein environment can exert a positive effect on its activity (rate) and productivity (total turnover number = TON).

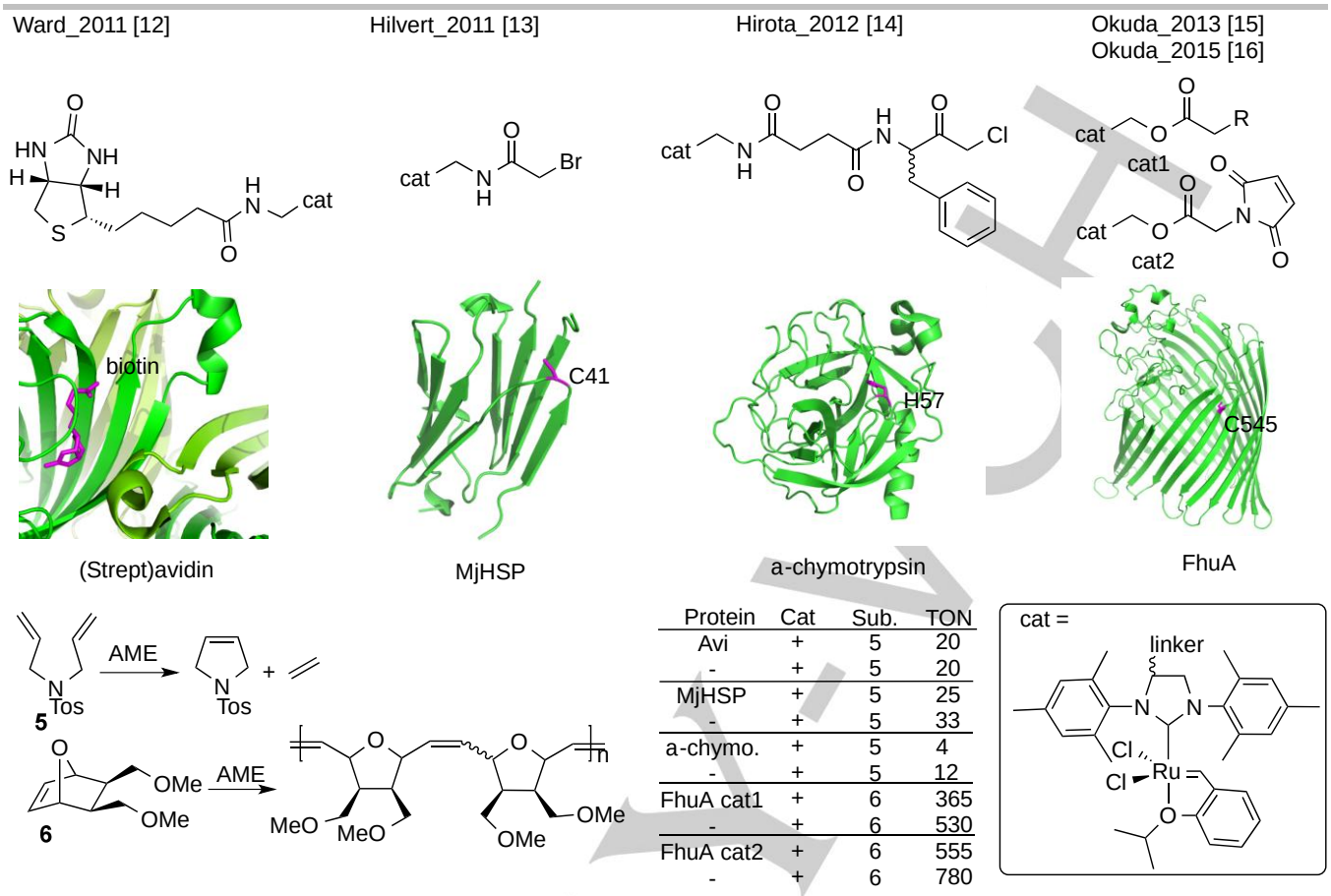

Protein	Cat	Sub.	TON
Avi	+	5	20
-	+	5	20
MjHSP	+	5	25
-	+	5	33
a-chymo.	+	5	4
-	+	5	12
FhuA cat1	+	6	365
-	+	6	530
FhuA cat2	+	6	555
-	+	6	780

Figure 2. Artificial Metathesases

In one of the first reports, Ward and coworkers linked the complex to D-biotin via its NHC backbone and incorporated the resulting construct into avidin which has a very high affinity for D-biotin ($K_d = 10^{-14}$ M, Figure 2).[12] Under acidic conditions and in the presence of high concentrations of $MgCl_2$ (0.5 M) – beneficial presumably thanks to reduced catalyst coordination to surface residues – the hydrophobic substrate *N*-tosyl diallyl amine **5** (TDA hereafter) was transformed into *N*-tosyl-3-pyrroline by ring-closing metathesis with a total turnover number of up to 20, comparable to the catalyst in the absence of the host protein.

Hilvert and coworkers chose the small heat shock protein MjHSP to anchor the ruthenium catalyst covalently via a cysteine (G41C) residue introduced in a strategic position at the rim of the β-barrel protein.[13] With TDA as substrate, the hybrid catalyst performed best under acidic conditions (pH 2.0) but with a slightly reduced TON (25) relative to the free catalyst (33).

Hirota and coworkers applied a “trojan horse” covalent coupling strategy to incorporate the ruthenium catalyst into α-chymotrypsin.[14] For this purpose they attached the catalyst via a glutamate linker to a hydrophobic peptide substrate motif of the serine protease. The C-terminal end of the peptide was modified to a chloroacetate group which enabled covalent-bond formation between the cofactor and the Ser side chain of the catalytic triad in the protein active site. The resulting hybrid catalyst yielded up to 4 turnover for substrate TDA under neutral conditions, in the presence of KCl and at only 25 μM catalyst concentration. However, the free cofactor was more productive (TON = 12) under identical conditions.

The Grubbs-Hoyveda 2nd generation catalyst can also be used for ring-opening olefin polymerization (ROMP). Okuda and coworkers tethered the catalyst to the β-barrel pore protein FhuA via an engineered Cys at the entry of the pore.[15,16] Successful attachement was confirmed by MS and a TON of up to 955 was reached with substrate 7-oxanorbornene **6**, about the same as with the Ru catalyst alone. The *cis/trans* selectivity was moderately affected by the protein (70:30 for the free catalyst vs 60:40 for the hybrid catalyst).

These examples demonstrate the tolerance of the Grubbs-Hoyveda catalyst for protein conjugation. However, no protein dependent rate acceleration was yet observed in any of the studies. It remains to be investigated whether initial metathesase designs can be optimized through protein engineering techniques.

3.2. C-H, N-H, S-H Insertion Reactions

While the AME designs in the last chapter were based on covalent or supramolecular anchoring of an artificial metallocofactor within a rigid protein scaffold, the examples in

the following exploit the principle of enzyme repurposing to create novel enzymatic function.

Proteins containing an iron porphyrin prosthetic group are very diverse and highly abundant in Nature. They serve several functions such as electron transport, small molecule binding and redox catalysis.[17] Cytochromes P450s catalyze among other transformations the hydroxylation of aliphatic or aromatic C–H bonds. In these reactions, an intermediate ferryl moiety (Fe(IV)-oxo, compound 1) which is generated from O_2 and two electrons, is the oxidizing species which cleaves a substrate C–H bond by hydrogen atom abstraction. The groups of Arnold and Fasan have now demonstrated that formal Fe(IV)-carbenoid and Fe(IV)-nitrenoid compounds, which are isoelectronic to Fe(IV)-oxo, are generated in various heme proteins and insert into C–H, N–H and S–H bonds. These C-C, C-N and C-S bond-forming reactions catalyzed by designed metalloenzymes are valuable since they proceed in water, at room temperature and are very stereoselective which is difficult to achieve with chemical catalysts.[18–20] The following carbene and nitrene transfer reactions have been described to be catalyzed by the iron porphyrin proteins: i) carbene transfer: cyclopropanation,[21–26] amination,[27,28] sulfidation,[29] ii) nitrene transfer: sulfamination,[30–33] sulfimination,[34] oxazolidinone formation.[35]

Cylcopropanation, amination, sulfidation:

To form the Fe(IV)-carbenoid intermediate, low spin ferric heme must be reduced into low spin ferrous heme prior to reaction with a diazo compound, e.g. ethyl diazoacetate (EDA hereafter). The Fe(IV)-carbenoid can undergo reaction with various aromatic nucleophiles such as i) olefins (e.g. styrene) to form cyclopropanes,[21–26] ii) prim. or sec. anilines to form sec. or tert. anilines[27,28] or iii) thiols to form sulfides.[29]

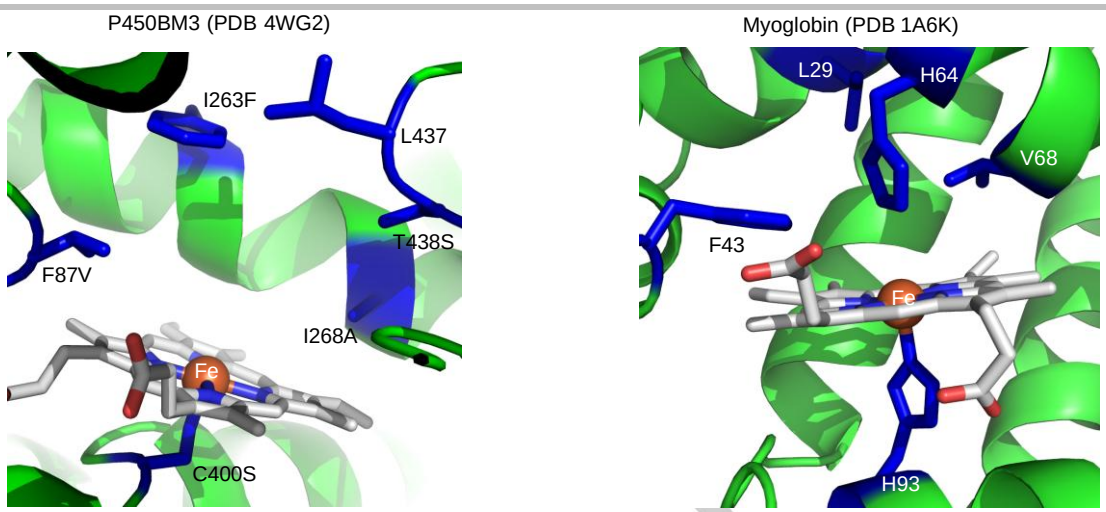

	Catalyst	TON	ee (%)	*trans/cis*	
a)	hemin	175	rac	86:14	wcb
	$P411_{BM3}$-CIS	67800	99 (cis)	10:90	
	BSA + hemin	349	7 (cis)	91:9	pe
	HSA + hemin	567	15 (cis)	91:9	
	CYP119-C316S	345	40 (cis)	20:80	
	CYP153A6-C363S	441	rac	90:10	
	TxtE	178	36 (cis)	70:30	
	Mb-H64V-V68A	46800	99.9 (trans)	99.1:0.9	
b)	$P450_{BM3}$-C400H-T268A-L437W-V78M-L181V	~8000	92	2:98	wcb
c)	$P450_{BM3}$-CIS	433			pe
	Mb-H64V-V68A	6150			
d)	Mb-H64V-C29A	2550			pe
e)	$P411_{BM3}$-T268A	250	89		wcb
	$P411_{BM3}$-CIS	680	60		
f)	Mb-H64V	200			pe
	Mb (Mn porphyrine)	140			
	Mb (Co porphyrine)	60			
g)	$P411_{BM3}$-CIS-T438S-I263F	361	97	ß/a 95:5	wcb
	$P411_{BM3}$-T268A-F87A	187	99	5:95	
h)	$P411_{BM3}$-CIS-I263A-T438S	320		er 18:82	pe
i)	CYP102A-FL#62	100			pe

pe = purified enzyme, wcb = whole cell bioconversion

Figure 3. Heme enzymes for C-H, N-H, S-R insertion reactions.

In cyclopropanation, diastereoselectivity and enantioselectivity is induced by the protein environment e.g. in the reaction between styrene and EDA. For the free hemin the (*rac*)-*trans*-cyclopropane is formed preferentially (86:14). With hybrid catalyst $P450_{BM3}$ mutant $P411_{BM3}$-CIS (which contains thirteen mutations including an axial Ser ligand) the *cis*-cyclopropane is produced (10:90) in high enantiopurity (ee_{cis} 99% (1*R*,2*S*), Figure 3a).[26]

Besides $P450_{BM3}$ i) other cytochrome P450s such as CYP119, CYP153 or TxtE,[22] ii) heme protein myoglobin[21] and even iii) non-heme proteins in the presence of hemin catalyze the reaction.[22] Every protein displays a different reactivity and selectivity (Figure 3a).

Mutation of the axial Cys to Ser shifts the Soret band of the protein ferrous-CO complex from 450 to 411 nm (hence the name P411 of the constructs). It also decreases the redox potential of $Fe^{III/II}$ from E°´= -420 mV to E°´= -293 mV so that the reduction of the ferric low spin resting state is possible either with sodium dithionide (E°´=-660 mV) and with NADPH (E°´=-320 mV, all potentials vs. SHE).[26] This allows the reaction to proceed *in cellulo*. Whole cell *E. coli* biotransformation with $P411_{BM3}$-CIS yielded > 60'000 TON .

Decreasing the electron density at the Fe(IV)-carbenoid facilitates the nucleophilic attack of styrene. This is achieved by replacement of the axial thiolate ligand steming from Cys or the alkoxide ligand stemming from Ser for less electron-rich amino acid side chains such as the phenolate of Tyr, the imidazole of His, or by removing the axial ligand altogether as realized in an Ala mutant. Indeed, $P450_{BM3}$-axHis performed best in whole cell cyclopropanation of styrene and EDA.[25] $P450_{BM3}$-axMet yielded second most product followed by Tyr>Ala>Ser>Cys which was essentially inactive. Myoglobin which bears His in the axial position, is a very good cyclopropantation catalyst yielding a TON of more than 45'000.[21]

While styrene is a good substrate, electron-deficient *N,N*-diethyl-2-phenylacrylamide was expected to be a poor nucleophile for Fe(IV)-carbenoid attack. The product of this reaction is a precursor of levomilnacipran, a potential drug to treat depression. Of the axial mutants initially tested, $P450_{BM3}$T268A-axHis was the best catalyst for this substrate with a TON of 7100 and 94 % *cis*-selectivity but only moderate enantioselectivity (42 % ee).[25] To improve the ee, active site residues were targeted for saturation mutagenesis. Mutant $P450_{BM3}$T268A-axHis-L437W-V78M-L181V was found to produce levomilnacipran precursor with 98 % *cis*-selectivity, 92 % ee and at a very high rate of more than 1000 turnover min^{-1} (~8000 TON), Figure 3b. Working under aerobic conditions is not detrimental to the yield with this mutant anymore, which might be related to the high reaction rate.

Besides olefins, nitrogen and sulfur nucleophiles have been successfully employed for the reaction with the Fe(IV)-carbenoid. While cytochrome $P450_{BM3}$-CIS yields a TON of 433 in the reaction of EDA with aniline, the myoglobin variant H64V-V68A leads to a TON of 6150.[27,28] Recently, Fasan and coworkers demonstrated a carbene insertion into S-H bonds with myoglobin.[29] Thioaniline yields a TON of 2550 with EDA. Ethyl 2-diazopropionate reacts with thioanillin to yield after rearrangement ethyl 2-thioanillinpropionate.

Sulfonamides, sulfimides and oxazolindinones:

Besides reactions proceeding through presumed Fe(IV)-carbenoids, intermediate Fe(IV)-nitrenoids are likely formed by reaction of ferrous low spin iron porphyrin protein with sulfonylazides or carbonazidates. The intermediates can undergo intramolecular C-H insertion to form cyclic benzosultams or can form sulfimides in an intermolecular reaction with sulfide nucleophiles (Figure 3e-h).

The cyclization of 2,4,6-triethyl-benzene-1-sulfonylazide proceeds best using $P411_{BM3}$-CIS-T438S which includes fourteen mutations including a Ser as an axial heme ligand instead of Cys.[30] This mutant yields the corresponding benzosultam with a TON of 383 and 73 % ee. The reaction can be carried out *in cellulo* to yield a TON of up to 430 and an improved *ee* of 87 % (Figure 3e).

Besides $P450_{BM3}$ other heme proteins such as horse radish peroxidase and myoglobin have been reported by Fasan and coworkers to catalyze intramolecular C-H sulfamination with TONs of 311 and 181, respectively (Figure 3f).[31]

As an alternative to sulfonylazides, carbonazidates have been employed yielding oxazolidinones in the presence of cytochrome CYP102A1 with a TON of 20 (Figure 3i). [35]

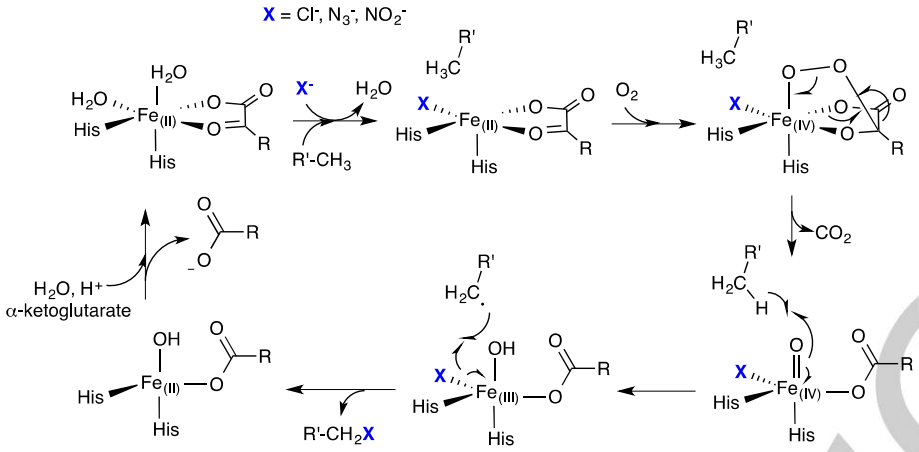

Figure 4. Proposed catalytic mechanism of non-heme iron halogenase SyrB2 with natural substrate chloride and surrogates N_3^- and NO_2^-.

The intramolecular sulfamination reaction is believed to proceed through abstraction of a hydrogen by the nitrene intermediate and subsequent radical rebound reaction.[35] If the protein has only little control over substrate positioning, hydrogen abstraction should occur from the weaker benzylic (bond dissociation energy, BDE, 85 kcal/mol) rather than the stronger homobenzylic (BDE 98 kcal/mol) alkyl C-H bond by the nitrene. In principle, reshaping the enzyme active site could trigger hydrogen abstraction from the stronger homobenzylic C-H group. This was tested with substrate 2-propyl-5-ethylcarbonyl-benzene-1-sulfonylazide.[32] It was found through saturation mutagenesis of various active site residues that variant $P411_{BM3}$-CIS-I263F-T438S has strong β-selectivity (95:5) whereas $P411_{BM3}$-CIS-T268A-F87A has strong α-selectivity (5:95). The reactions proceed with excellent enantioselectivity (Figure 3g).

Intermolecular C-H sulfamination has not been achieved yet. However, it was demonstrated that sulfide nucleophiles react with nitrenes in an intermolecular fashion. 4-methylbenzene sulfonylazide in reaction with methylphenylsulfide yields the corresponding sulfimides with up to 300 TON and 64 % ee (Figure 3h).[34]

Alkane nitration:

Halogenation of C-H bonds is carried out in Nature mostly by oxidative enzymes that belong to one of the three classes: i) heme-dependent haloperoxidases, ii) vanadium-dependent haloperoxidases and iii) non-heme iron α-ketogluterate-dependent haloperoxidases.[36] In the resting state of non-heme iron haloperoxidases ferrous iron is coordinated by two His, two H_2O and α-ketogluterate (Figure 4). In the putative catalytic cycle the equatorial H_2O is replaced by a halide ion. Upon substrate binding, the axial H_2O is replaced by O_2. The Fe(III)-dioxy compound rearranges in an oxidative decarboxylation to form Fe(IV)-oxo. This species can abstract a hydrogen from the substrate C-H to form Fe(III)-OH. The alkyl radical undergoes a radical rebound reaction with the halide ligand to form the alkyl halide product and Fe(II). Succinic acid is replaced by another molecule α-ketogluterate to close the catalytic cycle.[37,38]

It has now been shown by Bollinger and coworkers that the halide ligand can be replaced by nitride or azide ions which equally to halides can undergo a radical rebound reaction with the intermediate substrate radical in non-heme iron halogenase SyrB2.[39] Even though only a single turnover could be performed with this enzyme, improvement of the catalyst can be imagined by means of protein engineering.

3.3. Light-Driven Redox Reactions

With respect to renewable energy sources it is highly desirable to apply cheap reductants in concert with photocatalysts for the generation of high-energy (e.g. H_2) and added-value compounds.[40] In Nature, diiron dithiolate hydrogenases catalyze H_2 evolution formally from two electrons and two protons with a very high rate of >100'000 min^{-1}.[41] However, it is difficult to prepare this multidomain enzyme in large quantities for cheap H_2 production. Various groups have attempted to develop smaller derivatives of natural hydrogenases based on the immobilization of synthetic cofactors inside scaffold proteins or by modification of natural hydrogenase.[42–45]

Photocatalytic Artificial Metalloenzyme

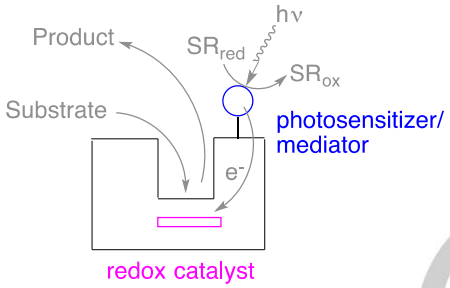

	Protein	redox catalyst	photosensitizer/mediator	Reaction	TON	initial rate [min^{-1}]	Ref.
a)	P450$_{BM3}$heme	hemin	[Ru((OMe)$_2$bpy)$_2$(PhenA)]$^{2+}$	Alkyl-H ⟶ Alkyl-OH	935	125	Cheruzel_2013 [48]
b)	MoFeP	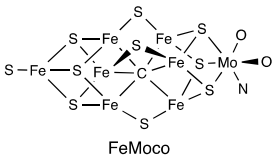 FeMoco	[Ru(bpy)$_2$(PhenA)]$^{2+}$	HCN + 6 H$^+$ + 6 e$^-$ ⟶ CH$_4$ + NH$_3$ 2H$^+$ + 2 e$^-$ ⟶ H$_2$ C$_2$H$_2$ + 2H$^+$ + 2 e$^-$ ⟶ C$_2$H$_4$	~9 ~70 ~98	0.059	Tezcan_2012 [46] Tezcan_2011 [47]
c)	18aa-cyt c556	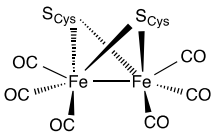	[Ru(bpy)(tpy)im$_{His}$]$^{2+}$	2H$^+$ + 2 e$^-$ ⟶ H$_2$	~9	0.19	Hayashi_2012 [49]
d)	HYDA	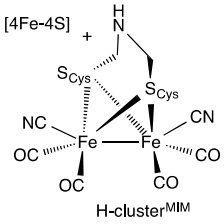 H-cluster^{MIM}	Photosystem I (+ plastocyanin)	2H$^+$ + 2 e$^-$ ⟶ H$_2$	ND	~100000	Happe_2013 [51]
e)	swMb	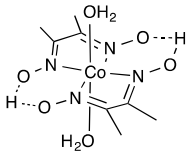	[Ru(bpy)$_3$]$^{2+}$ 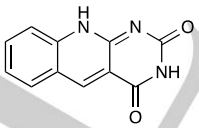	2H$^+$ + 2 e$^-$ ⟶ H$_2$	3 (7)* 5 (8.3)*		Artero_2014 [52]
f)	nitrobindin	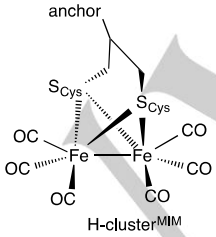 H-cluster^{MIM}	[Ru(bpy)$_3$]$^{2+}$	2H$^+$ + 2 e$^-$ ⟶ H$_2$	~130 (~130)*	~2.3	Hayashi_2014 [50]
g)	flavodoxin	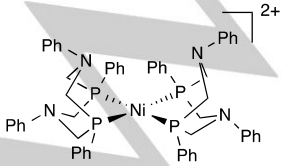	Photosystem 1 (+ cyt c$_6$)	2H$^+$ + 2 e$^-$ ⟶ H$_2$	2825	75	Utschig_2013 [53]

* = without protein

Figure 5: Photocatalytic artificial metalloenzymes.

Nitrogenase catalyzes the six electron reduction of N_2 into two equivalents of NH_3. In the reaction, one equivalent of H_2 is

formed as a byproduct. The enzyme complex consists of two components, the iron protein (FeP) and the molybdenum-iron protein (MoFeP). The MoFeP contains two metal clusters with FeMoco being the reaction center. Electrons are shuttled from FeP into MoFeP under consumption of 16 ATP molecules per molecule N_2. To uncouple the enzyme from the costly ATP consumption, Tezcan and coworkers developed a hybrid photocatalyst that contains the MoFeP as the redox catalyst and, instead of the FeP, includes a covalently anchored $[Ru(bpy)_2(PhenA)]^{2+}$ photosensitizer/mediator (PS/M hereafter) pair.[46,47] Under irradiation with visible light and with sodium dithionide as the sacrificial reductant, this hybrid enzyme catalyzes H_2 evolution, acetylene reduction and six-electron cyanide reduction (to methane) with multiple turnover (Figure 5b). A similar approach was followed by Cheruzel and coworkers in their attempt to uncouple the heme domain of hydroxylating enzyme cytochrome $P450_{BM3}$ from its reductase domain and thereby replace costly NADPH by sodium diethyldithiocarbamate as an electron source.[48] The catalytic heme domain was covalently functionalized with PS/M $[Ru((OMe)_2bpy)_2(PhenA)]^{2+}$. This hybrid system catalyzed hydroxylation of lauric acid with a TON of more than 900 (Figure 5a). Inspired by natural hydrogenases, Hayashi and coworkers developed a hybrid system consisting of a scaffold peptide comprising the 18 N-terminal amino acids of cytochrome c556, functionalized with a $[Fe_2(CO)_6]$ cluster bound to two Cys thiolates as the redox catalyst and His imidazole-tethered $[Ru(bpy)(typ)]^{2+}$ as PS/M.[49] This minimalistic hydrogenase model evolved H_2 with a TON of up to 9 (Figure 5c). In another design, the same group tethered the diirondithiolate catalyst $[(\mu\text{-}S)_2Fe_2(CO)_6]$ via a maleimide anchor to a Cys side chain of β-barrel protein nitrobindin. Even though no protein rate acceleration for H_2 evolution was observed, the diirondithiolate moiety is functional within this protein scaffold (TON = 130), Figure 5f.[50] The H-cluster, the reaction center of hydrogenase HYDA consist of a simple [2Fe-2S] cluster linked via a Cys bridge to the [2Fe] cluster that contains the diirondithiolate motive. In nature, maturation of the [2Fe]-cluster requires three additional enzymes,

HYDE, HYDF, HYDG. This sophisticated assembly renders the efficient heterologous production of hydrogenase difficult. However, Happe and coworkers have shown that a close synthetic mimic of the [2Fe] cluster can be added to apo-HYDA, which only contains the [2Fe-2S]-cluster, to obtain a hydrogenase (up to 100'000 turnover min^{-1}). The construct shows virtually no loss of activity vs. the natural enzyme in the light-driven protein reduction using photosystem I as the PS/M couple and ascorbate as a sacrificial reductant.[51] The apo-enzyme could be readily expressed in *E. coli*, Figure 5d.

As an alternative to diirondithiolate redox catalysts, cobaloximes have been investigated for H_2 evolution. Artero and coworkers functionalized apo-sperm whale myoglobin with two cobaloxime complexes.[52] The researchers assumed that coordination of cobaloxime to axial His93 generated the catalytically active species. In the presence of $[Ru(bpy)_3]^{2+}$ and ascorbate a TON of 3 for the production of hydrogen was observed. The free cobaloxime, however, had slightly better reactivity, Figure 5e.

Nickel complex $[Ni(P_2PhN_2Ph)_2]^{2+}$ is another excellent H_2 evolution catalyst. Utschig and coworkers have introduced this catalyst into a hybrid system with photosystem I as host protein. In the presence of ascorbate as sacrificial reductant, it evolves H_2 with a TON of 3000, Figure 5g.[53]

4. New Scaffolds

In the last decade a growing number of protein scaffolds have been used to design AMEs. Here we present the latest reports in respect to scaffold diversity.

Peptide dendrimers resemble proteins in their polymeric Nature but are generally structurally less well-defined and hence more flexible. This additional flexibility can be considered as an additional design challenge for hybrid catalysts. Reymond and coworkers presented a peptide dendrimer with a $[Fe(bpy)_3]^{2+}$ core that displayed peroxidase activity. The amino acid decoration surrounding the iron core led to a 10-fold rate acceleration compared to $[Fe(bpy)_3]^{2+}$.[54]

Bacterial pore FhuA is a large beta-barrel protein. It has been employed by Hayashi and Schwaneberg to create covalent AMEs for Ru-catalyzed metathesis[15] and Rh-catalyzed phenylacetylene polymerization.[55] Although similarly active, tethering of the CpRh(COD) catalyst to the protein altered the *cis/trans* selectivity of the polymerization towards 47:53 vs. 93:7 for the free catalyst.

Metallothioneins are Cys-rich proteins responsible for the storage of mono- and divalent metal ions such as Fe^{II}, Co^{II}, Ni^{II} and others. The 32-amino acid metallothionein α-domain known to bind a 4-metal ion cluster by interactions with 11 Cys residues, was prepared by solid-phase peptide synthesis and incubated with $FeCl_2$ by Hayashi and coworkers.[56] In single turnover experiments this reducing agent was able to effect single electron reduction of Mb and the four-electron reduction of diazo compound methyl red into two equivalents of aniline. Nitrobindin is a heme-binding bacterial β-barrel protein which can accommodate synthetic catalysts linked covalently via cysteine residues. Hayashi and coworkers used this strategy to incorporate $[CpRh(COD)]^+$ and investigated phenylacetylene polymerization. With a crystal structure of the catalyst at hand, the authors selected residues in proximity to the metal for mutagenesis studies. The *cis:trans* ratio of the polymeric product is significantly influenced by the protein environment. One mutant showed 82% enrichment of the *trans*-product whereas the free catalyst was highly *cis*-selective (93:7).[57] Lewis and coworkers used the same scaffold to incorporate a $[Mn(tpy)]^{2+}$ complex and tested benzylic oxidation. In the presence of peroxyacetic acid, benzylic methylene groups were oxidized into carbonyls and styrene into phenyl epoxide.[58] Ueno and coworkers applied a β-helical protein nanotube equipped with Cys residues to covalently attach a bipyridine ligand to bind the water compatible Lewis acid Sc^{3+}. This hybrid catalyst was employed in the enantioselective ring opening of *cis*-stilbene epoxide with aniline as a nucleophile.[59] Ricoux and coworkers used xylanase as a scaffold to bind Mn^{III}-*meso*-tetrakis(*p*-carboxyphenyl)-porphyrin and Mn^{III}-salen with micromolar affinity. These catalysts were successfully applied in the oxidation of styrene derivatives with oxone as the stoichiometric oxidant.[60]

Neocarcinostatin has been shown to bind a testosterone-conjugated iron porphyrin complex. The hybrid complex was used by Ricoux and coworkers to oxidize sulfides into sulfoxides using H_2O_2. However, the protein decelerated the reaction and only 13 % ee was observed.[61]

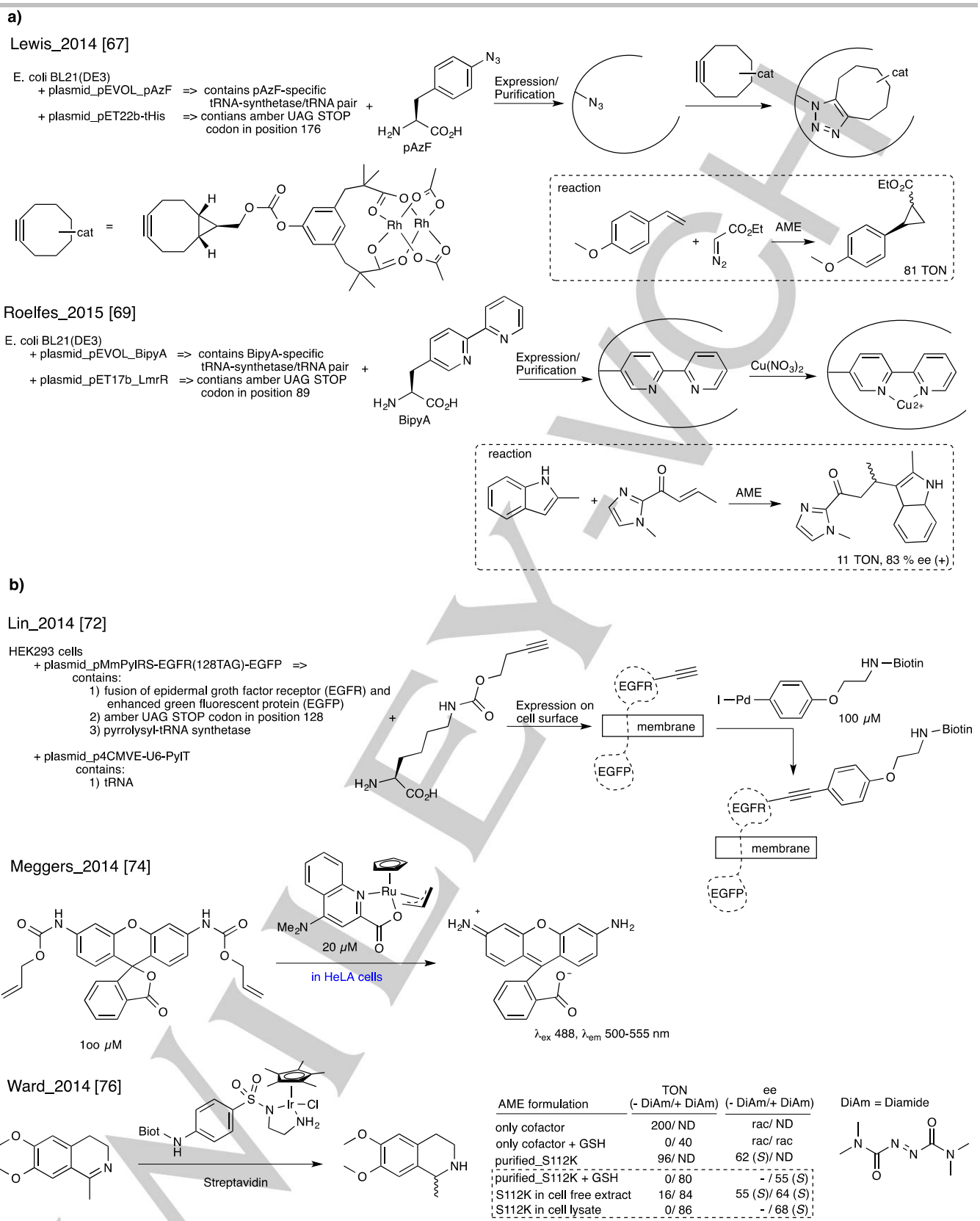

Figure 6. Novel anchoring strategies for synthetic metallocofactors within proteins (a) and *in vivo* applications of transition metal catalysts (b).

RNase A contains an *N*-terminal α-helix (S-peptide) which can be cleaved off yielding a stable residual protein called S-protein. Upon mixing of the S-protein with the S-peptide, full nuclease

activity is restored. Inspired by a study by Imperiali and coworkers[62], Sträter and coworkers, equipped the S-peptide with His residues in strategic positions to enable selective binding of the fragment Cp*RhCl and Cp*IrCl. The hybrid catalyst showed low enantiomeric induction and protein rate acceleration in the transfer hydrogenation of cyclic imines.[63] Human carbonic anhydrase II binds aryl sulfonamide inhibitors with nanomolar affinity. In a supramolecular strategy, Ward and coworkers tethered complex [Cp*IrCl(pico)] to benzylsulfonamide which results in a catalyst that binds to hCAII with low nanomolar affinity. In imine transfer hydrogenation, the hybrid catalyst showed up to 70% ee for the *S*-amine product which was produced with a TON of 9 at 4 °C (40 TON at 40 °C).[64]

A novel protein dimer, LmrR, was used as scaffold by Roelfes and coworkers to covalently attach a phenantroline ligand. When incubated with Cu^{II}, an active Diels-Alderase was obtained that could be optimized by genetic modification of the active site to produce up to 97% ee and a TON of 33 in the reaction of cyclopentadiene with α,β-unsaturated acylpyridine.[65] The protein scaffold accelerated the reaction almost 5-fold. The same catalyst displayed hydratase activity for the same enone substrate employed as a dienophile in the Diels-Alder reaction with up to 84 % ee.[66]

5. New Anchoring Methods

Finding the right anchoring strategy is crucial to building an efficient AME from a protein scaffold and a metal catalyst. Traditionally, three anchoring methods have been used: covalent, supramolecular and dative anchoring. Covalent anchoring relies on the incorporation of reactive Cys in a strategic position within the protein cavity. However, limited labeling selectivity often requires Cys-to-Ala mutation to prevent undesired modifications on native Cys residues. To overcome this problem, Lewis and coworkers have exploited an orthogonal, highly specific strategy for catalyst incorporation.[67] Using the amber stop codon, they genetically introduced the unnatural amino acid (UAA hereafter) *p*-azido-Phe in a cavity within the thermostable protein tHisF and coupled it to a cyclooctyne-functionalized dirhodium catalyst via a strain-promoted click reaction. The hybrid catalyst was active in the cyclopropanation of styrene with EDA but no protein rate acceleration was observed, Figure 6a.

Roelfes and coworkers followed a strategy described earlier by Schultz.[68] Using the amber stop codon strategy they incorporated the bipyridinyl-Ala UAA into the protein LmrR (Figure 6a).[69] Upon addition of Cu^{II}, the hybrid catalyst was active in the asymmetric Friedel-Crafts alkylation of indole with an enone electrophile. Genetic optimization of active site residues yielded a mutant that produced the product with 83 % ee and a TON of 11.

6. In vivo Application of Transition Metal Catalysts

With respect to future applications of AMEs in artificial metabolic pathways it is essential to identify methods to ensure the catalytic activity of transition metals *in vivo*. Many cellular components such as glutathione (GSH) can coordinate and deactivate transition metal catalysts. In recent years, numerous transition metal mediated reactions have been shown to function under biological conditions, albeit with low productivity rarely exceeding a few turnovers.[70,71]

Lin and coworkers used Pd-catalyzed Suzuki coupling to label proteins on mammalian cell surfaces (Figure 6b).[72] Bradley and coworkers carried out Pd-catalyzed Suzuki coupling inside cells.[73] Meggers and coworkers demonstrated the alkylating activity of a Ru piano stool complex *in vivo* (Figure 6b).[74] Sadler and coworkers used various transition metal piano stool complexes in human cancer cell lines as catalysts to shift the equilibrium between $NADP^+$ and NADPH towards NADPH which triggered cell death. The IC_{50} of the transition metal complex of < 5 μM in the presence of 2 mM sodium formate were determined.[75] These are encouraging reports with respect to applications of AMEs *in vivo*.

Ward and coworker observed that artificial transfer hydrogenases based on Noyori-type biotinylated iridium piano stool catalysts are inactive in *E. coli* lysates which hampers the establishment of high-throughput genetic screening assays.[76] They recently demonstrated that, upon diamide-triggered oxidation of glutathione, the AMEs remain functional in cell free extracts and even in cell lysates, Figure 6b.

7. Enzyme Models

The oxygen transporter sperm whale myoglobin is a small heme protein. It can be readily expressed in *E. coli* and has been used as an engineering platform for novel catalytic activities such as sulfoxidation[77] and hydroxylation.[78] In an seminal study, Lu and coworkers demonstrated that introduction of a His facial triad and a Glu into myglobin in the close proximity to the heme moiety allows binding of a second iron and leads to emergent nitric oxide reductase activity.[79,80] The structurally characterized model confirmed the successful design. Heme-copper oxidases are heme proteins that contain a Cu center in the proximity to the iron heme center. An additional feature of the heme-copper oxidase active site is an unusual, conserved covalent link between a neighboring Tyr-Cε and an His-Nε. The specific role of this Tyr-His dimer in dioxygen reduction is unresolved. Wang, Lu and coworkers set out to investigate this functionality by introducing the UAA Tyr-Cε-imidazole in position F33 of Cu_BMb, a myoglobin construct with an additional engineered copper binding site. This protein displays significant active-site similarity with heme-copper oxidase.[81] Upon addition of Cu^{II} to this mutant, the rate of water production increased 4-fold vs. a control that contained the Cu^{II} but only Tyr in position 33. Surprisingly, the absence of Cu^{II} did not significantly diminish oxidase activity. However, the frequency of production of reactive oxygen species (superoxide and peroxide) as side products decreased significantly upon addition of Cu^{II}. A TON of >1000 was observed for this enzyme. In a related study, Lu and coworkers examined whether positioning the active Tyr residue in another position than F33 relative to the Cu_B side in myoglobin Cu_BMb could improve oxidase activity. Mutant G65Y-Cu_BMb turned out to be a much better oxidase than F33Y-Cu_BMb producing at least 1000 turnovers.[82]

In the next study, the group investigated if the oxidase activity of Cu_BMb-F33Y can be further improved by systematic tuning of the Fe-Cu redox potential.[83] While natural heme-copper oxidases have redox potentials varying between -59 and +365 mV that of model Cu_BMb-F33Y is +95 mV. It was speculated that increasing this value would correlate with an improved O_2 reduction activity. To test this hypothesis, residue S92 which forms an H-bond with axial His93 was chosen for mutagenesis into Ala: increased hydrophobicity at this position was expected to increase the redox potential. Gratifyingly, mutant Cu_BMb-S92A-F33Y has a redox potential of +123 mV. Next, the heme prosthetic group was targeted for derivatization to increase the redox potential. Heme *a* carries an extended sesquiterpene substituent and has been reported to have an increased redox potential vs. heme *b,* the cofactor in heme-copper oxidase, that contains a vinyl group in the same position. Since supplementation of Cu_BMb-F33Y with heme *a* yielded insoluble protein, heme derivatives with the alternative electron-withdrawing substituents acetyl and formyl were prepared and incubated with Cu_BMb-F33Y. The resulting diformyl-substituted heme *b* inside Cu_BMb-F33Y yielded an AME with a redox potential of +320 mV, almost as high as that of bovine heart heme-copper oxidase (+365 mV). The increased redox potential correlates with an O_2 reduction rate enhancement of nearly 10-fold vs. heme *b* loaded Cu_BMb-F33Y. The reaction mechanism of heme-copper oxidase dioxygen reduction is believed to involve an intermediate tyrosyl radical at the Tyr-His residue in the active site. Using model Cu_BMb-F33Y Lu and coworkers demonstrated by EPR measurements that a Tyr radical can indeed be observed as a short-lived reaction intermediate.[84]

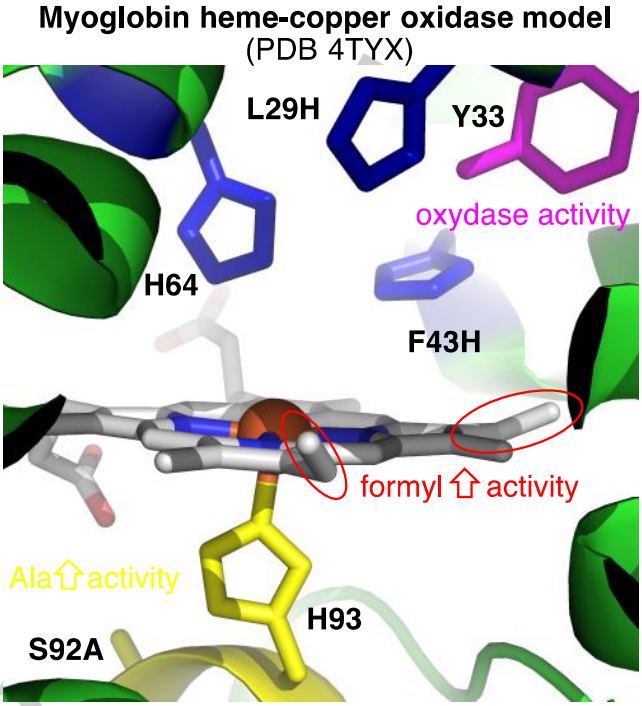

Figure 7. Crystal structure of heme-copper oxidase model Cu_BMb_F33Y.

8. Conclusion and Outlook

Today, chemistry is striving for “greener” reaction processes which are more economical, energy-saving and environmentally benign. At the same time there is a need for the light-driven production of high-energy compounds as renewable energy sources from cheap and abundant starting materials. As implied in this microreview, AMEs that combine biomolecular with chemical diversity might offer solutions to these pressing demands. Initially, AMEs were designed as isolated entities to modify the selectivity and activity of catalytically active metal species.[85,86] While the optimization of AMEs by genetic and chemical means is far from accomplished, one aims now at employing AMEs in cascade reactions in concert with chemo- and biocatalysts and ultimately in synthetic biological systems.[87] The protein scaffold offers a particular protective microenvironment for functional metal centers and AMEs are accordingly promising candidates for interfacing synthetic chemical with biological processes.[88] The strategy of natural metalloenzyme repurposing benefits from its genuine *in vivo* compatibility but is likely limited in the accessible reaction repertoire.[89] In contrast, the approach of embedding artificial metallocofactors into protein scaffolds holds the promise to enable a wide variety of catalytic abiological reaction types *in*

vivo. However, present hybrid catalysts and in particular their artificial prosthetic groups are often characterized by a limited *in vivo* compatibility. Tezcan and coworkers have demonstrated that a catalytic Zn^{II} cofactor can generate an artificial hydrolase in the *E. coli* periplasm.[7] While this is higly encouraging, it will be crucial to develop strategies that allow even larger multiatomic metallocofactors to assemble with their protein partners *in cellulo* to form functional AMEs. Ultimately, the creation of machinery for artificial metallocofactor biosynthesis and assembly with the scaffold protein would be desirable.

Acknowledgements

The authors would like to thank Dr. Valentin Köhler for his precious help in preparing this review.

Keywords: artificial metalloenzymes • enzyme repurposing • light-driven redox reactions • enzyme models • protein engineering

(1) Yu, F.; Cangelosi, V. M.; Zastrow, M. L.; Tegoni, M.; Plegaria, J. S.; Tebo, A. G.; Mocny, C. S.; Ruckthong, L.; Qayyum, H.; Pecoraro, V. L. *Chem. Rev.* **2014**, *114*, 3495.

(2) Lewis, J. C. *ACS Catal.* **2013**, *3*, 2954.

(3) Aoki, S.; Kimura, E. *Compreh. Coord. Chem. II* **2004**, *8*, 601.

(4) Zastrow, M. L.; Pecoraro, V. L. *Biochemistry* **2014**, *53*, 957.

(5) Zastrow, M. L.; Peacock, A. F. a; Stuckey, J. a; Pecoraro, V. L. *Nat. Chem.* **2012**, *4*, 118.

(6) Der, B. S.; Edwards, D. R.; Kuhlman, B. *Biochemistry* **2012**, *51*, 3933.

(7) Song, W. J.; Tezcan, F. A. *Science* **2014**, *346*, 1525.

(8) Rufo, C. M.; Moroz, Y. S.; Moroz, O. V; Stöhr, J.; Smith, T. a; Hu, X.; DeGrado, W. F.; Korendovych, I. V. *Nat. Chem.* **2014**, *6*, 303.

(9) Khare, S. D.; Kipnis, Y.; Greisen, P.; Takeuchi, R.; Ashani, Y.; Goldsmith, M.; Song, Y.; Gallaher, J. L.; Silman, I.; Leader, H.; Sussman, J. L.; Stoddard, B. L.; Tawfik, D. S.; Baker, D. *Nat. Chem. Biol.* **2012**, *8*, 294.

(10) Grela, K.; Gułajski, Ł.; Skowerski, K. In *Metal-Catalyzed Reactions in Water*; Wiley VCH, **2013**; pp. 291–336.

(11) Tomasek, J.; Schatz, J. *Green Chem.* **2013**, *15*, 2317.

(12) Lo, C.; Ringenberg, M. R.; Gnandt, D.; Wilson, Y.; Ward, T. R. *Chem. Commun.* **2011**, *47*, 12065.

(13) Mayer, C.; Gillingham, D. G.; Ward, T. R.; Hilvert, D. *Chem. Commun. (Camb).* **2011**, *47*, 12068.

(14) Matsuo, T.; Imai, C.; Yoshida, T.; Saito, T.; Hayashi, T.; Hirota, S. *Chem. Commun. (Camb).* **2012**, *48*, 1662.

(15) Philippart, F.; Arlt, M.; Gotzen, S.; Tenne, S.-J.; Bocola, M.; Chen, H.-H.; Zhu, L.; Schwaneberg, U.; Okuda, J. *Chemistry (Easton).* **2013**, *19*, 13865.

(16) Sauer, D. F.; Bocola, M.; Broglia, C.; Arlt, M.; Zhu, L.; Brocker, M.; Schwaneberg, U.; Okuda, J. *Chem. Asian J.* **2015**, *10*, 177.

(17) Smith, L. J.; Kahraman, A.; Thornton, J. M. *Proteins Struct. Funct. Bioinforma.* **2010**, *78*, 2349.

(18) Lebel, H.; Marcoux, J.-F.; Molinaro, C.; Charette, A. B. *Chem. Rev.* **2003**, *103*, 977.

(19) Nicolas, I.; Le Maux, P.; Simonneaux, G. *Coord. Chem. Rev.* **2008**, *252*, 727.

(20) Hyster, T. K.; Arnold, F. H. *Isr. J. Chem.* **2015**, *55*, 14.

(21) Bordeaux, M.; Tyagi, V.; Fasan, R. *Angew. Chemie Int. Ed.* **2014**, *54*, 1744.

(22) Heel, T.; McIntosh, J. A.; Dodani, S. C.; Meyerowitz, J. T.; Arnold, F. H. *Chembiochem* **2014**, *15*, 2556.

(23) Renata, H.; Wang, Z. J.; Kitto, R. Z.; Arnold, F. H. *Catal. Sci. Technol.* **2014**, *4*, 3640.

(24) Coelho, P. S.; Brustad, E. M.; Kannan, A.; Arnold, F. H. *Science* **2013**, *339*, 307.

(25) Wang, Z. J.; Renata, H.; Peck, N. E.; Farwell, C. C.; Coelho, P. S.; Arnold, F. H. *Angew. Chem. Int. Ed.* **2014**, *53*, 6810.

(26) Coelho, P. S.; Wang, Z. J.; Ener, M. E.; Baril, S. A.; Kannan, A.; Arnold, F. H.; Brustad, E. M. *Nat. Chem. Biol.* **2013**, *9*, 485.

(27) Sreenilayam, G.; Fasan, R. *Chem. Commun.* **2014**, *51*, 1532.

(28) Wang, Z. J.; Peck, N. E.; Renata, H.; Arnold, F. H. *Chem. Sci.* **2014**, *5*, 598.

(29) Tyagi, V.; Bonn, R. B.; Fasan, R. *Chem. Sci.* **2015**, *6*, 2488.

(30) McIntosh, J. A.; Coelho, P. S.; Farwell, C. C.; Wang, Z. J.; Lewis, J. C.; Brown, T. R.; Arnold, F. H. *Angew. Chem. Int. Ed.* **2013**, *52*, 9309.

(31) Bordeaux, M.; Singh, R.; Fasan, R. *Bioorg. Med. Chem.* **2014**, *22*, 5697.

(32) Hyster, T. K.; Farwell, C. C.; Buller, A. R.; McIntosh, J. a; Arnold, F. H. *J. Am. Chem. Soc.* **2014**, *136*, 15505.

(33) Singh, R.; Bordeaux, M.; Fasan, R. *ACS Catal.* **2015**, *4*, 546.

(34) Farwell, C. C.; Mcintosh, J. A.; Hyster, T. K.; Wang, Z. J.; Arnold, F. H. *J. Am. Chem. Soc.* **2014**, *136*, 8766.

(35) Singh, R.; Kolev, J. N.; Sutera, P. A.; Fasan, R. *ACS Catal.* **2015**, *5*, 1685.

(36) Vaillancourt, F. H.; Yeh, E.; Vosburg, D. a.; Garneau-Tsodikova, S.; Walsh, C. T. *Chem. Rev.* **2006**, *106*, 3364.

(37) Matthews, M. L.; Neumann, C. S.; Miles, L. A.; Grove, T. L.; Booker, S. J.; Krebs, C.; Walsh, C. T.; Bollinger, J. M. *Proc. Natl. Acad. Sci.* **2009**, *106*, 17723.

(38) Wong, S. D.; Srnec, M.; Matthews, M. L.; Liu, L. V; Kwak, Y.; Park, K.; Bell, C. B.; Alp, E. E.; Zhao, J.; Yoda, Y.; Kitao, S.; Seto, M.; Krebs, C.; Bollinger, J. M.; Solomon, E. I. *Nature* **2013**, *499*, 320.

(39) Matthews, M. L.; Chang, W.; Layne, A. P.; Miles, L. A.; Krebs, C.; Bollinger, J. M. *Nat. Chem. Biol.* **2014**, *10*, 209.

(40) Lee, S. H.; Kim, J. H.; Park, C. B. *Chem. Eu. J.* **2013**, *19*, 4392.

(41) Lubitz, W.; Ogata, H.; Ru, O.; Reijerse, E. *Chem. Rev.* **2014**, *114*, 4081.

(42) Caserta, G.; Roy, S.; Atta, M.; Artero, V.; Fontecave, M. *Curr. Opin. Chem. Biol.* **2015**, *25*, 36.

(43) Onoda, A.; Hayashi, T. *Curr. Opin. Chem. Biol.* **2015**, *25*, 133.

(44) Utschig, L. M.; Soltau, S. R.; Tiede, D. M. *Curr. Opin. Chem. Biol.* **2015**, *25*, 1.

(45) Winkler, J. R.; Gray, H. B. *Chem. Rev.* **2014**, *114*, 3369.

(46) Roth, L. E.; Tezcan, F. A. *J. Am. Chem. Soc.* **2012**, *134*, 8416.

(47) Roth, L. E.; Tezcan, F. A. *ChemCatChem* **2011**, *3*, 1549.

(48) Tran, N.-H.; Nguyen, D.; Dwaraknath, S.; Mahadevan, S.; Chavez, G.; Nguyen, A.; Dao, T.; Mullen, S.; Nguyen, T.-A.; Cheruzel, L. E. *J. Am. Chem. Soc.* **2013**, *135*, 14484.

(49) Sano, Y.; Onoda, A.; Hayashi, T. *J. Inorg. Biochem.* **2012**, *108*, 159.

(50) Onoda, A.; Kihara, Y.; Fukumoto, K.; Sano, Y.; Hayashi, T. *ACS Catal.* **2014**, *4*, 2645.

(51) Esselborn, J.; Lambertz, C.; Adamska-Venkatesh, A.; Simmons, T.; Berggren, G.; Noth, J.; Siebel, J.; Hemschemeier, A.; Artero, V.; Reijerse, E.; Fontecave, M.; Lubitz, W.; Happe, T. *Nat. Chem. Biol.* **2013**, *9*, 607.

(52) Bacchi, M.; Berggren, G.; Niklas, J.; Veinberg, E.; Mara, M. W.; Shelby, M. L.; Poluektov, O. G.; Chen, L. X.; Tiede, D. M.; Cavazza, C.; Field, M. J.; Fontecave, M.; Artero, V. *Inorg. Chem.* **2014**, *53*, 8071.

(53) Silver, S. C.; Niklas, J.; Du, P.; Poluektov, O. G.; Tiede, D. M.; Utschig, L. M. *J. Am. Chem. Soc.* **2013**, *135*, 13246.

(54) Geotti-bianchini, P.; Darbre, T.; Reymond, J. *Org. Biomol. Chem.* **2013**, *1*, 344.

(55) Onoda, A.; Fukumoto, K.; Arlt, M.; Bocola, M.; Schwaneberg, U.; Hayashi, T. *Chem. Commun.* **2012**, *48*, 9756.

(56) Sano, Y.; Onoda, A.; Sakurai, R.; Kitagishi, H.; Hayashi, T. *J. Inorg. Biochem.* **2011**, *105*, 702.

(57) Fukumoto, K.; Onoda, A.; Mizohata, E.; Bocola, M.; Inoue, T.; Schwaneberg, U.; Hayashi, T. *ChemCatChem* **2014**, *6*, 1229.

(58) Zhang, C.; Srivastava, P.; Ellis-Guardiola, K.; Lewis, J. C. *Tetrahedron* **2014**, *70*, 4245.

(59) Inaba, H.; Kanamaru, S.; Arisaka, F.; Kitagawa, S.; Ueno, T. *Dalton Trans.* **2012**, *41*, 11424.

(60) Allard, M.; Dupont, C.; Muñoz Robles, V.; Doucet, N.; Lledós, A.; Maréchal, J.-D.; Urvoas, A.; Mahy, J.-P.; Ricoux, R. *Chembiochem* **2012**, *13*, 240.

(61) Sansiaume-Dagousset, E.; Urvoas, A.; Chelly, K.; Ghattas, W.; Maréchal, J.-D.; Mahy, J.-P.; Ricoux, R. *Dalton Trans.* **2014**, *43*, 8344.

(62) Imperiali, B.; Roy, R. S. *J. Am. Chem. Soc.* **1994**, *116*, 12083.

(63) Genz, M.; Köhler, V.; Krauss, M.; Singer, D.; Hoffmann, R.; Ward, T. R.; Sträter, N. *ChemCatChem* **2014**, *6*, 736.

(64) Monnard, F. W.; Nogueira, E. S.; Heinisch, T.; Schirmer, T.; Ward, T. R. *Chem. Sci.* **2013**, *4*, 3269.

(65) Bos, J.; Fusetti, F.; Driessen, A. J. M.; Roelfes, G. *Angew. Chem. Int. Ed.* **2012**, *51*, 7472.

(66) Bos, J.; García-Herraiz, A.; Roelfes, G. *Chem. Sci.* **2013**, *4*, 3578.

(67) Yang, H.; Srivastava, P.; Zhang, C.; Lewis, J. C. *Chembiochem* **2014**, *15*, 223.

(68) Lee, H. S.; Schultz, P. G. *J. Am. Chem. Soc.* **2008**, *130*, 13194.

(69) Drienovská, I.; Rioz-Martínez, A.; Draksharapu, A.; Roelfes, G. *Chem. Sci.* **2014**, *6*, 770.

(70) Völker, T.; Meggers, E. *Curr. Opin. Chem. Biol.* **2015**, *25*, 48.

(71) Soldevila-Barreda, J. J.; Sadler, P. J. *Curr. Opin. Chem. Biol.* **2015**, *25*, 172.

(72) Li, N.; Ramil, C. P.; Lim, R. K. V; Lin, Q. *ACS Chem. Biol.* **2015**, *10*, 379.

(73) Yusop, R. M.; Unciti-Broceta, A.; Johansson, E. M. V; Sánchez-Martín, R. M.; Bradley, M. *Nat. Chem.* **2011**, *3*, 239.

(74) Völker, T.; Dempwolff, F.; Graumann, P. L.; Meggers, E. *Angew. Chem. Int. Ed.* **2014**, *53*, 10536.

(75) Soldevila-Barreda, J. J.; Romero-Canelón, I.; Habtemariam, A.; Sadler, P. J. *Nat. Commun.* **2015**, *6*, 6582.

(76) Wilson, Y. M.; Dürrenberger, M.; Nogueira, E. S.; Ward, T. R. *J. Am. Chem. Soc.* **2014**, *136*, 8928.

(77) Carey, J. R.; Ma, S. K.; Pfister, T. D.; Garner, D. K.; Kim, H. K.; Abramite, J. a; Wang, Z.; Guo, Z.; Lu, Y. *J. Am. Chem. Soc.* **2004**, *126*, 10812.

(78) Oohora, K.; Kihira, Y.; Mizohata, E.; Inoue, T.; Hayashi, T. *J. Am. Chem. Soc.* **2013**, *135*, 17282.

(79) Yeung, N.; Lin, Y.-W.; Gao, Y.-G.; Zhao, X.; Russell, B. S.; Lei, L.; Miner, K. D.; Robinson, H.; Lu, Y. *Nature* **2009**, *462*, 1079.

(80) Lin, Y.; Wang, J.; Lu, Y. *Sci. China Chem.* **2014**, *57*, 346.

(81) Liu, X.; Yu, Y.; Hu, C.; Zhang, W.; Lu, Y.; Wang, J. *Angew. Chem. Int. Ed.* **2012**, *51*, 4312.

(82) Miner, K. D.; Mukherjee, A.; Gao, Y.-G.; Null, E. L.; Petrik, I. D.; Zhao, X.; Yeung, N.; Robinson, H.; Lu, Y. *Angew. Chem. Int. Ed.* **2012**, *51*, 5589.

(83) Bhagi-damodaran, A.; Petrik, I. D.; Marshall, N. M.; Robinson, H.; Lu, Y. *J. Am. Chem. Soc.* **2015**, *136*, 11882.

(84) Yu, Y.; Mukherjee, A.; Nilges, M. J.; Hosseinzadeh, P.; Miner, K. D.; Lu, Y. *J. Am. Chem. Soc.* **2014**, *136*, 1174.

(85) Wilson, M. E.; Whitesides, G. M. *J. Am. Chem. Soc.* **1978**, *100*, 306.

(86) Levine, H. L.; Kaiser, E. T. *J. Am. Chem. Soc.* **1978**, *100*, 7670.

(87) Denard, C. a.; Hartwig, J. F.; Zhao, H. *ACS Catal.* **2013**, *3*, 2856.

(88) Köhler, V.; Wilson, Y. M.; Dürrenberger, M.; Ghislieri, D.; Churakova, E.; Quinto, T.; Knörr, L.; Häussinger, D.; Hollmann, F.; Turner, N. J.; Ward, T. R. *Nat. Chem.* **2013**, *5*, 93.

(89) Renata, H.; Wang, Z. J.; Arnold, F. H. *Angew. Chemie Int. Ed.* **2015**, *54*, 3351.